Advanced signal processing techniques for wind turbine gearbox bearing failure detection

Journal:	*WCCM 2017*
Manuscript ID	CM-MFPT-0277-2017.R1
Topic:	Condition monitoring (CM) methods and technologies
Date Submitted by the Author:	28-Apr-2017
Complete List of Authors:	Esmaeili, Kamran; University of Southampton, Engineering and Environment Zuercher, Manuel; Process Machinery and System Engineering,
Keywords:	Acoustic emission, Electrostatic, Signal processing, Bearing

Advanced signal processing techniques for wind turbine gearbox bearing failure detection

K. Esmaeili*[1], M. Zuercher[2], L. Wang[1], T.J. Harvey[1] and W. Holweger[3]

[1]National Centre for Advanced Tribology, University of Southampton, SO17 1BJ, Southampton, UK
[2]Process Machinery and System Engineering, Friedrich-Alexander-University, Erlangen, Germany
[3]Schaeffler Technologies AG & Co. KG, Herzogenaurach, Germany

Premature wind turbine gearbox failure has been observed to occur after periods as short as 5 years, while the design life of a gearbox is expected to exceed 20 years [1]. Most wind turbine failures have been found to be initiated at the bearings [2]. The formation of white etching cracks (WECs) on the subsurface of bearings can occur after 6 months to 2 years of operation [3]. WECs, which can eventually lead to spallation and catastrophic failure of the wind turbine gearbox, have been identified as one of the most severe damaging causes of failure in bearings.

Recent research has suggested that electrical load is one of the key parameters affecting the formation of WECs. To investigate the characteristics and formation of WECs, a test rig was designed at the University of Erlangen-Nuremberg. The rig facilitated the simultaneous data capture of vibration, electrostatic and acoustic emission through dedicated sensors.

Signal processing techniques have been utilised to process and correlate sensor data in order to detect WECs before the final failure occurs and trace back to earlier stages of propagation. This conference paper demonstrates the effectiveness of the suggested signal processing techniques, using multiple sensors, to detect and monitor bearing crack initiation and propagation.

References

[1] Ragheb, A. Ragheb, 2010. Wind Turbine Gearbox Technologies. Amman, Jordan, Proceedings of the 1st International Nuclear and Renewable Energy Conference (INREC10).

[2] Sheng, S., 2015. Wind Turbine Gearbox Reliability Database, Condition Monitoring, and O&M Research Update. Golden, Colorado, National Laboratory of the U.S. Department of Energy (NREL).

[3] Evans, M.-H., 2016. An updated review: white etching cracks (WECs) and axial cracks in wind turbine gearbox bearings. Materials Science and Technology, Volume 32:11, pp. 1133-1169.

*Corresponding author; email: ke3g11@soton.ac.uk; Tel.: +44 (023) 8059 3166.

Advanced signal processing techniques for wind turbine gearbox bearing failure detection

K Esmaeili Mainauthor[1], M Zuercher Coauthor[2], L Wang Coauthor[1], T Harvey Coauthor[1], W Holweger Coauthor[1], N White Coauthor[1], E Schlücker Coauthor[2]
1 National Centre for Advanced Tribology, University of Southampton, SO17 1BJ, UK, kamran.esmaeili@soton.ac.uk
2 Process Machinery and System Engineering, Friedrich-Alexander-University, Germany

Abstract

The reliability of bearing failure in gearboxes, caused by White Etching Cracks (WEC) is one of the major concerns in wind turbine industry. Recent publications have suggested that electrical load is considered to be one of the key parameters affecting the formation of cracks in wind turbine bearings, especially in the case of WECs which might be formed as early as 6 months[1-2]. Despite the major developments over the past two to three decades, the mechanisms of WEC formation in rolling element bearings are still not understood. This is due to the complexity of the factors that influence WEC formation such as speed, load (mechanical and electrical) and lubrication, as well as lack of effective monitoring techniques and signal processing methods that extract the signals relevant to WEC.

To investigate the formation of WECs under the influence of electrical load, a test rig was designed which facilitates the simultaneous data capture of electrostatic (ES) and acoustic emission (AE) through dedicated sensors in a systematic approach. The physical findings related to WEC failures in the bearings and basic analysis of the sensor signals are reported in a parallel paper. This paper presents the results of WEC sensing using ES and AE using a time-frequency analysis method, where correlations between the electrostatic charge signals with other sensor measurements are found to have the potential in identifying WEC initiation and propagation due to electric loading applied to the bearings.

1. Introduction

WEC is one of the mechanisms that causes a large number of bearing failures in wind turbine gearboxes[2-4]. WECs formation mechanisms have been widely discussed over the past decades, however their drivers are still unclear. WECs eventually causes failure through surface spalling but is often traced to their origin in bearing subsurface of up to 1.5 mm in depth. Figure 1 shows an optical image of a subsurface contained WEC in a bearing race obtained from this study. More information about the characteristics of WECs can be found in the literature[5-7]. While the root causes of WEC are still unclear, one of the hypotheses suggested by Loos *et al.*[1] and Holweger *et al.*[2] is the continuous material alterations induced by current or electromagnetic fields. They suggested that[12]:

- Self-charging of lubricants in the ball-raceway contact leads to the occurrence of a transient current flow.

- The transient current flow induces a local electrical polarisation near the surface. A sudden discharge may resulting the transfer of the current from the bearing surface into subsurface defect domains.
- This produces a thermal effect inside the defect domains, causing additional material alteration combining relocation of carbon, chromium and hydrogen in and around the defect domains.
- The local thermal stress, caused by such straying currents leads to a local increase in strain and subsequently stress in the subsurface. The induced stress will be the cause of new hotspots for further electrical loading and thus accelerate the strain. Locally stressed sites in the material will be the cause of atoms migration and local diffusion that creates an instability of the stressed site. Overcoming a stress limit, the subsurface hotspot will create local relaxation by formation of area with redistribution of carbon, chromium and silicon.
- The accumulation of plastic deformation and distorted microstructure eventually leads to a sudden burst of significant damages.

In parallel to the majority of research focusing on investigation of WEC root causes through physical analysis of materials, a number of sensors have been installed on the bearing test rig used to create WEC in this study to develop sensing techniques that can detect WEC formation at early stages, including an acoustic emission (AE) sensor, electrostatic (ES) sensor as well as temperature, oil flow rate and load sensors. Common bearing sensing techniques such as vibration sensors have shown the ability in detecting cracks and their propagation in wind turbine gearboxes[8-9], but are not able to detect WEC in real time at its early formation stages. Vibration, although extremely useful in many cases, is insensitive to subtle effects such as cracks at their initiation and early growth stages. In the case of WECs that are originated in bearing subsurface, vibration monitoring will not be effective until the crack is manifested to a surface damage[2].

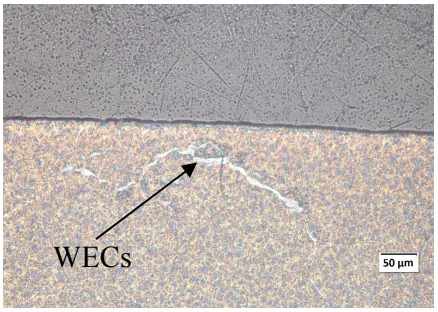

Figure 1. An optical image of a WEC observed in the bearing from Test A (more details are given in Table 1).

A recent study by Barteldes *et al.*[10] has used AE sensors to identify the acoustic waves in materials that undergo irreversible microstructural changes. They found that acoustic wave energy increases with the formation of both surface and subsurface cracks. They also showed that AE sensor was able to detect signatures that can be related to WEC through the monitoring of crack growth and surface bulging due to formation of White Etching Area (WEA) in the subsurface of the bearing.

Electrostatic sensors (ES) have shown to be able to detect bearing failures based on charge detections and thus have been chosen in this study to investigate their feasibility of detecting WECs. ES sensors can detect electrostatic charges generated in both dry

and lubricated tribological contacts due to surface charge[11-15], tribocharging[1516] and wear debris generation[17,19]. In the cases of bearings, ES sensors have shown to be able to detect early spalling and debris in the lubricant[11-12, 18-19]. This paper presents the results of ES and AE sensing focusing on developing advanced signal processing techniques that support WEC root cause investigation and enable early detection of WEC formation.

2. Experimental details

Details of the test rig, the bearing and test programme is given in a parallel paper at this conference authored by Zuercher *et al.*[20]. Here a brief introduction is given to highlight the sensing system and the tests discussed in this paper.

2.1. Experimental rig

Figure 2 shows a schematic of the bearing test rig where multiple sensors are installed, including ES, AE and infrared sensors, to monitor the main parameters that are considered to affect the bearing life. The ES and AE sensors are positioned between the bearings and close to the end of one bearing respectively (see Figure 3). The ES and AE sensors are used to monitor discharges originated from the bearings, crack initiation and lubricant degradation as well as their correlations for WEC detection.

Within the bearing test rig, deep grove ball bearings (DGBB, size 6203) with martensitic hardened SAE 52100 steel grade are axially loaded.

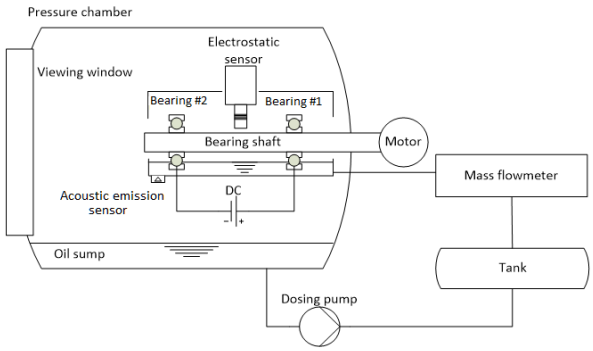

Figure 2. A schematic of the bearing test rig at the Institute of Process Machinery and System Engineering, Erlangen, Germany.

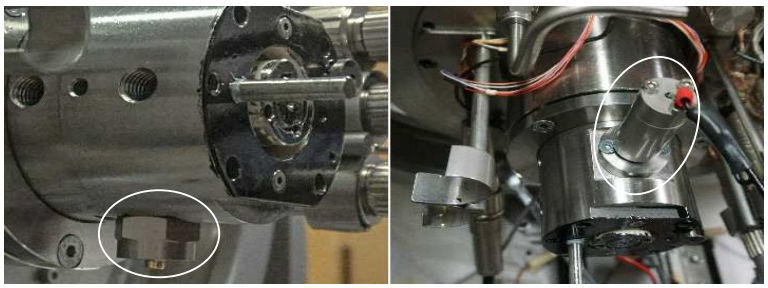

Figure 3. The AE (left) and ES (right) sensors located on (and at the end of) the motor shaft and between the two test bearings respectively.

2.2. The tests

In this paper, results from three bearing tests are presented. Details of these tests are given in Table 1.

Table 1. Parametric conditions for the three tests A, B and C.

	Test A	**Test B**	**Test C**
Total running time (h)	19.3	142.6	39.4
Axial force measured (N)	1800-2100	2000-2250	1803-2232.5
WEC	In bearing #1 inner ring	In bearing #1 inner ring	No WECs observed
Pressure	Ambient		
Speed (1/min)	4500		
Voltage (V)	0-15	0-15 (step approach)	0-15
Lubricant volume flow rate (mL/min)	3.4	0-0.5h: 5.5 -> 3.4 16-22h: 1 22-end: 3.4	0-15.15h: 3.4 15.15-end: 40 -> 7.2

During the tests, the gas pressure in the test chamber, and the shaft rotating speed were kept constant, while the potential applied and the lubricant flow rate were varied (except Test A where the flow rate was kept at 4 mL/min throughout the test). The axial load was also initially set at 1800 N for all the tests. However, as the bearings expand due to the increase in temperature, the axial force measured varies throughout the tests (more details can be found in the paper by Zuercher *et al.*[20]).

In all these tests, a potential was applied to the bearings to accelerate the formation of WECs, more information on the approach and the values is given in the paper by Zuercher *et al.*[20].

The parametric conditions for Test A, have been used previously in multiple tests, all resulted in WECs[20]. Test B was a replication of Test A, with the difference that the voltage was applied in a step approach, by increase the voltage by 1V every 24 hours, to investigate the intensity of the potentials applied on WECs formation. In addition, the lubricant flow rate was reduced to 1 mL/min for 6 hours to accelerate the failure. Finally, Test C was conducted in a similar condition as in Test A, with the difference that at 15 hours (when the first signatures of a failure were observed in Test A), the lubricant volume flow rate was increased to avoid the formation of WECs.

3. Signal analysis approach

When a crack is initiated on/below the surface of a bearing raceway, acoustic wave energy is released at a regular interval due to the impact of the rolling elements and the raceway. Similarly, electrostatic charge generation can be also cyclic. The ES and AE signals are thus processed using the data acquisition device developed by QASS GmbH, which enables the online FFT monitoring of the bearings throughout the test. The sampling rate was set at 1.5625 MHz for the tests. This sampling rate has previously used in detecting WECs at the institute of Process Machinery and System Engineering, Erlangen and has proven to be effective (more on the sampling rate in Results section).

A time-frequency analysis has been implemented in this study to investigate the frequency variations over time of the signals. A Short-Time-Fourier-transformation (STFT) was employed as it is a computationally efficient method, which has previously been used to detect signatures of a WEC failure event using acoustic emission signals[10]. Hence, STFT of the signals are calculated:

$$STFT\{x[n]\}(m,\omega) \equiv \mathrm{X}(m,\omega) = \sum_{-\infty}^{\infty} x[n]\omega[n-m]e^{-j\omega n} \quad (1)$$

Where $x[n]$ is the signal, $\omega[n]$ is the window. In this case, m is discrete and ω is continuous. The window is moved by a quarter of the sample frame at each stage. The output amplitude values are arbitrary because of a combination of the sensors output values in mV and preamplifier-factor, so these values do not carry any physical meanings.

The output signals from the sensors are then fed into the following equation to magnify the small amplitudes and increase the reliability of the analysis as well as a reduction in storage size from 24 bits to 16 bits:

$$a = (\log_2(a_0 + 2^{lw}) - lw)(\frac{2^{16}}{23 - lw}) \quad (2)$$

Where, lw is defined as the logarithmic value, a_0 is the output signal from the FFT operation and a is the output signals of the AE and ES signals presented in Results section. Here, the logarithmic value is defined as 14. This method was previously proven the ability to detect signatures of WECs formation[10].

4. Results

Primary analysis of the AE and ES signals using STFT method has shown that the energy is dominated by the frequencies below 50 kHz for all the tests. In these regions, there is a significant increase in the energy level when approaching a failure, in Test A and Test B. In addition, no important features were observed in the frequencies higher than 100 kHz. For Test A, there are four distinct regions, which together can provide valuable information on the health state of the rolling element bearings, identified as follows:

- Region 1: Start-up region, in which the heat generated from the rotating components, is translated into an increase in the axial load. No voltage is applied and little to no discharges observed.
- Region 2: Discharge region, where the potential is applied to accelerate WECs formation, resulting in an increase in the discharge level measured at the bearings.
- Region 3: self-regulating region, where the ES sensor, due to the fluid film formation, measures minimum discharges, while the AE sensor detects an increase in the acoustical waves.
- Region 4: Running-to-failure region that is identified by a sudden and continuous increase in the ES and AE signals, until the end of the test.

In Region 1 (before the potential was applied at 3 hours), there has not been any substantial discharge generations. During this period, the temperature of the bearings increased from 20 to 100 °C due to the friction between the balls and raceways. This

rise in temperature caused the bearings to expand, which results in an increase in the axial load measured. Immediately after the test is started, the AE signals detected a sudden change in the acoustical waves due to the insufficiency of the fluid film (hydrodynamic) formed to prevent the impacts of the balls and raceways. As the test continues, more tribofilms form causing less surface impacts between the balls and the raceways and a reduction in the acoustical waves measured.

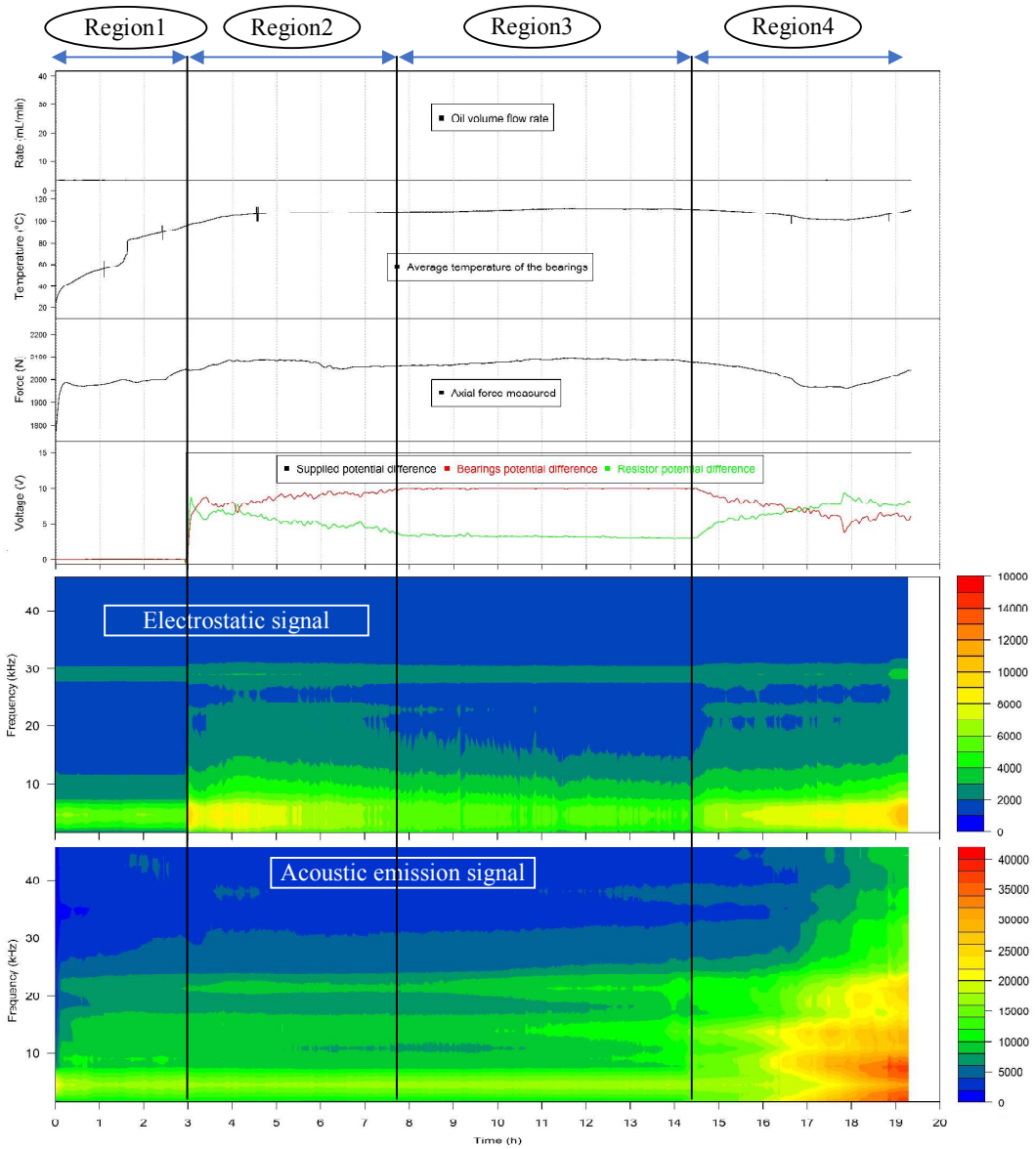

Figure 4. Test A sensor data plotted in line with each other.

Region 2 immediately starts after the voltage is set to 15 V at 3 hours. The increase in potentials applied, results in the flow of a current from balls to the raceways generating discharges within the bearings, which are detected in the ES signals at 4.57 kHz, more information on the mechanism is given by Zuercher *et al.*[20]. The AE signals also show an increase in the energy level at the frequency band of 21 kHz, which can be associated

with the microstructural activities taking place within the materials. These discharges reduce over time due to the further formation of the tribofilm between the balls and the raceways, which continues until the end of Region 2.

Region 3 starts when the discharge level reaches a state of equilibrium in discharge generation identified in the ES signals between 7.5 to 14.5 hours. During this period, the AE signals show steady increase in the energy across 7.62, 13.7 and 21 kHz frequency bands. Barteldes *et al*.[2,10] has previously shown that these increases in the energy level for the AE signals can be related to the formation of WECs by accumulation of plastic deformations within the defect domains.

Region 4 starts when both the AE and ES signals show a sudden increase followed by a gradual and continuous rise in their energy levels. It is not yet clear what causes this sudden rise in the ES signals as it previously reached an equilibrium state. However, by observing the AE signals, this can be concluded that these sudden discharges are caused by the damages made to the tribofilm as the result of cracks propagation or other mechanisms featured in the AE signals. The ES signals detect features of a failure at 4.57 kHz while the AE signals detects these features at four different frequency bands of 3.09, 7.62, 13.7 and 21 kHz, with the first two frequency bands having the highest energy.

Test A has demonstrated the correlation between the induced currents and WECs formation by showing the generation of discharges prior to the detection of acoustical waves. These results comply with the findings from Loos *et al*.[1] and Holweger *et al*.[2] on the formation of WECs by induced current described in Introduction of this paper.

Test B was conducted by applying the potential in a step approach, after a reduction from 15 to 6 V at 8 hours. The step approach was performed by increasing the potential by 1 V every 24 hours until reaching the discharge region. The intention behind this strategy was to observe the effect of various low-intensity potentials on the formation of WECs. Furthermore, between 16-22 hours the lubricant flow rate was set to 1 mL/min to investigate its effect on the acoustical energy detect by the AE signals and the failure. Similarly, the four regions discussed in Test A can be defined for Test B.

In Region 1 (Prior to the supplied potential at 3 hours), the temperature of the bearings increased from 40 to 110 °C due to friction between the balls and the raceways. Immediately after the test started, high acoustical energy can be observed at the frequency band of 4.57 kHz, which can be associated with the impacts of the balls and the raceways, as there was not enough time for the tribofilm to effectively form. During this period, The ES signals have detected higher discharge energy at 8000 in contrast to 6000 in Test A. The higher discharges can be associated with the change in the lubricant flow rate from 5.5 to 3.4 mL/min, immediately after the test has begun. Until the system fully accommodate this reduction in the lubricant flow rate, higher friction between the lubricant surfaces are present, causing higher discharges.

Region 2 starts when the potential is applied to the bearings at 3 hours. Following this, after the potential reaches 15 V around 7 hours, the magnitude of the ES signals increased sharply reaching 11000 in energy. Around 8 hours, the potential is reduced to 6 V until the end of Region 2 at 13 hours. Following this reduction, the magnitude of the ES energy is reduced strongly from 11000 to 8000, while at the same time, the AE signals show a gradual increase in the energy at the frequency band of 21 kHz.

Region 3 starts when the discharges reach a minimum level at 13 hours and ends at 101 hours. The AE and ES signals, prior to the reduction in the lubricant flow rate at 16.5

hours, show a steady increase in the energy levels. However, the reduction in the lubricant flow rate results in a rapid rise of the AE energy at 18 hours followed by a steady increase until the end of Region 3. Moreover, the ES signals also show a gradual increase in the energy between 18-25 hours, followed by a state of equilibrium until the end of Region 3. The increase in the AE signals can be associated with more intense impacts between the balls and the bearings, as no longer enough quantity of the lubricant is present to prevent these impacts. For ES signals, the discharges from the surface contacts within the lubricant is reduced due to the reduction in the flow rate, however more discharges are generated from the surface impacts which explains the steady increase in the ES signals. In Region 3, the applied potential increases every 24 hours by 1 V until reaching 10 V at 101 hours. The ES signals drop to the minimum level between 97-102 hours, which might be due to the faults within the system.

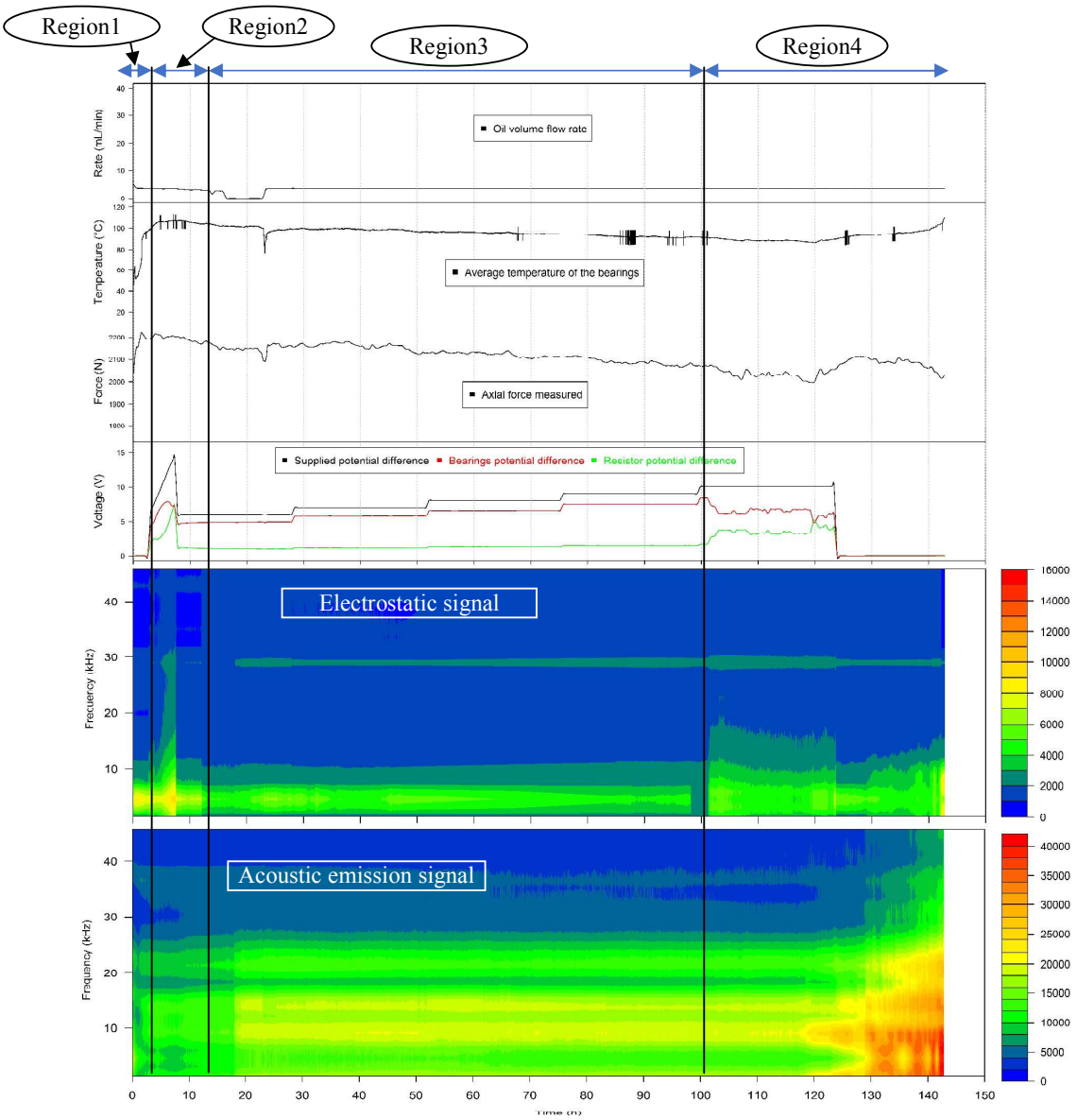

Figure 5. Test B sensor data plotted in line with each other. Voltage supply was cut-off at 123 h, thus a significant loss in discharges, followed by a period of steady increase in discharges.

Region 4 begins when the applied potential is set at 10 V around 101 hours. At 102 hours, the ES signals show a sharp increase in the energy level which is followed by a steady decrease until 123 hours. During the same period, the AE signals detected an increase across the frequency bands of 3.09, 7.62, 13.7 and 21 kHz. At 123 hours, the supplied potential is reduced to 0V to decelerate the formation of WECs. At this period, the ES energy reduced sharply around 123 hours due to the reduction in the applied potential. However, after a low discharge period, the ES signals suddenly surge simultaneously with the increase in the AE signals at 128 hours. Following this, the AE and ES signals show a gradual rise until the end of the test.

Microstructural observation of Test B has shown significantly less WECs in comparison to Test A. This can be justified by considering that the increase in the acoustical energy was not solely influenced by the discharges but also the lubricant volume flow rate. This suggests that the increase in the acoustical waves might have been due to the formation of surface cracks prior to WECs formation. Also, a lower potential values were applied during the test in comparison to Test A but over a longer period, which confirms the correlation between the intensity of the current and the formation of WECs. This complies with the hypothesis proposed by Loos *et al.*[1] and Holweger *et al.*[2] on the formation of WECs; by considering that a lower potential results in a more gradual migration of carbon, chromium and hydrogen in and around the defect domains. Furthermore, Test B has shown that it is not necessary for the applied potentials to exist in Region 4 for the bearings to fail. This can be due to the fact that WECs have already advanced into a critical stage, meaning there is no need for the accelerating conditions to exist. This stage can be associated with a number of plastic deformations inside the defect zones of the bearings, explained by Loos *et al.*[1] and Holweger *et al.*[2].

Test C was conducted in a similar setting to Test A, with the difference that the lubricant volume flow rate was increased from 3.4 to 40 mL/min at 15 hours followed by a gradual decrease until reaching 6 mL/min at the end of the test.

As Figure 6 shows, Test C is identical to Test A prior to the increase in the lubricant volume flow rate around 15 hours. After the volume flow rate increased from 3.4 to 40 mL/min, the system moves back into a discharge region (Region 2), instead of progressing into Region 4. This increase has prevented the bearings to reach the critical point at which the bearings enter Region 4. Immediately after the volume flow rate increased to 40 mL/min, the ES signals detect a steep increase in the discharge energy which can be due to the surface contacts the lubricants surfaces at higher flow rates. The AE signals also show a small increase in the energy level at the frequency band of 13.7 kHz. Furthermore, the temperature of the bearings is reduced, as the higher flow rate increases the speed at which the heat is transported from the bearings. This reduction in the temperature also reduces the axial load measured.

Similar to Region 2, Region 3 is also repeated in Test C. Region 3 is repeated as the self-regulating region is reappeared after Region 2 by a combination of the tribofilm formation and a reduction in the lubricant flow rate, causing a reduction in discharges at 33 hours.

Test C, unlike the other tests, does not reach the region with the intense plastic deformations and can be assumed to have repeating regions (Region 2 and 3). No WECs are observed at the end of the test and the AE signals do not detect any high-energy acoustical waves throughout the test. The maximum AE energy measured is at 15000

compared to 41000 of that in Test A and B. In the three tests, the ES signals are shown to provide the features of a failure at the frequency band of 4.57 kHz, while the AE signals show the features of a failure at four frequency bands of 3.09, 7.62, 13.7 and 21 kHz.

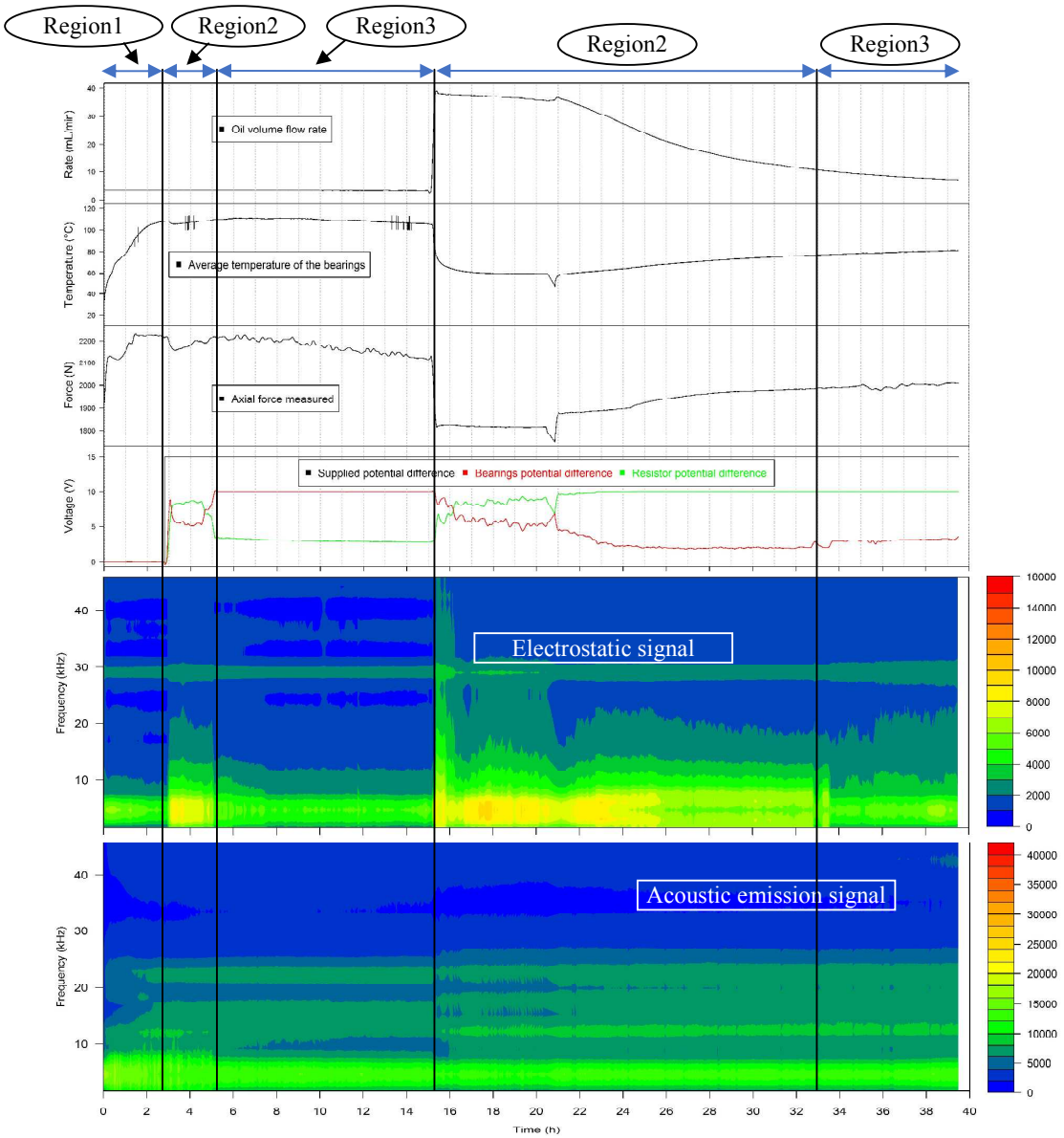

Figure 6. Test C sensor data plotted in line with each other. No region 4 is evident here as the discharges were not yet effective to reach the the critical level to cause intense plastic deformation.

These frequency bands are shown to be effective in defining the four regions and the likelihood of a failure event. The rise in the ES signals in these tests correlates with the electromagnetic fields generated as the result of a transient current and although cannot be directly associated with the state or the health of the bearings, it can provide valuable information regarding the conditions necessary for WECs formation and its propagation.

In this study, using multisensing methods, utilising AE and ES sensors, it was shown how STFT method could be an effective approach in detecting material defects and monitor the propagation of WECs.

5. Conclusions

WECs are formed by a sequence of events caused by a transient current flow through the bearings, leaving the defect zones vulnerable for the migration of carbon, chromium and hydrogen. This paper has shown the relationship between the electrical load and the discharges generated, resulting in WECs in rolling element bearings. It has also shown how STFT method can be utilised using multisensing techniques, utilising the AE and ES sensors, to detect the signatures of WECs in frequency region between 0-20 kHz. Further, it was shown how the features of a failure can be analysed to determine the health and the lifetime of the bearings as well as identifying the required conditions for the formation of WECs. Furthermore, it was demonstrated how the tests are classified into distinct regions each having different characteristics and the conditions necessary for the formation of WECs.

Further tests are crucial by altering the volume flow rate and applied potential, independent of each other, to gain a better understanding of the WECs mechanisms and verify the results discussed in this paper. The focus of the future papers will be on analysing the features by increasing the low frequency (0 to 50 kHz) resolution and comparing the effectiveness of signal processing methods such as continuous wavelet transform (CWT) to gain a better understanding of the phenomena.

Acknowledgements

The author would like to acknowledge Schaeffler Technologies AG & Co. KG, Germany, the Institute of Process Machinery and System Engineering in Erlangen, Germany and QASS GMBH Qualität Automation Systeme Software, Germany for their technical supports.

This research has been funded by University of Southampton and Schaeffler Technologies AG & Co. KG.

References and footnotes

1. Loos, J., Bergmann, I. and Goss, M. (2016) “Influence of Currents from Electrostatic Charges on WEC Formation in Rolling Bearings”, Tribology Transactions, 59:5, 865-875, DOI: 10.1080/10402004.2015.1118582
2. Holweger, W., Wolf, M., Merk, D., Blass, T., Goss, M., Loos, J., Barteldes, S. and Jakovics, A., 2015. White etching crack root cause investigations. Tribology Transactions, 58(1), pp.59-69
3. Luyckx, J. (2011), Hammering Wear Impact Fatigue Hypothesis WEC/ ir-WEA Failure Mode in Roller Bearings. Available at: http://www.nrel.gov/wind/pdfs/day2_sessioniv_3_hansen_luyckx.pdf.
4. Luyckx, J. (2012), “White Etching Crack Failure Mode in Roller Bearings: From Observation via Analysis to Understanding and an Industrial Solution,” Yoshimi, T. and William, M. (Eds.), Rolling Element Bearings, pp 1–25, ASTM International: Anaheim, CA.

5. Evans, M.-H. (2012), "White Structure Flaking in Wind Turbine Gearbox Bearings: Effects of Butterflies and White Etching Cracks (WECs)," Materials Science and Technology, 28(1), pp 3–18.
6. Evans, M.-H., et al. (2013), "Effect of Hydrogen on Butterfly and White Etching Crack (WEC) Formation under Rolling Contact Fatigue (RCF)," Wear.
7. Stadler, K. and Stubenrauch, A. (2017), "Premature Bearing Failures in Wind Gearboxes and White Etching Cracks", the SKF business and technology magazine, available at: http://www.powertransmission.com/issues/1014/Premature_Bearing-_Failures_PTE1014.pdf
8. Igba, J., Alemzadeh, K., Durugbo, C. and Eiriksson, E.T., 2016. Analysing RMS and peak values of vibration signals for condition monitoring of wind turbine gearboxes. Renewable Energy, 91, pp.90-106.
9. Siegel, D., Zhao, W., Lapira, E., AbuAli, M. and Lee, J., 2014. A comparative study on vibration-based condition monitoring algorithms for wind turbine drive trains. Wind Energy, 17(5), pp.695-714.
10. BARTELDES, S. and HOLWEGER, W., Using High-Frequency-Impulse-Measurement (HFIM) for Detection of Lubrication driven WEC-formation.
11. H.E.G. Powrie, R.J.K. Wood, T.J. Harvey and S. Morris, Re-analysis of electrostatic wear-site sensor data from FZG gear scuffing tests, Condition Monitor, 177 (Sept 2001) 6-12 (ISSN 0268-8050).
12. T.J. Harvey, R.J.K. Wood, G. Denuault and H.E.G. Powrie, Investigation of electrostatic charging mechanisms in oil lubricated tribo-contacts, Tribology International, 35(2002) 605-614.
13. J.E. Booth, K.D. Nelson, T.J. Harvey, R.J.K. Wood, L. Wang, H.E.G. Powrie and J.G. Martinez, "The feasibility of using electrostatic monitoring to identify diesel lubricant additives and soot contamination interactions by factorial analysis", Tribology International, Volume 39, Issue 12, December 2006, Pages 1564-1575.
14. J.E. Booth, T.J. Harvey R.J.K. Wood & H.E.G. Powrie, "Scuffing detection of TU3 cam-follower contacts by electrostatic charge condition monitoring", Tribology International, Volume 43, Issues 1-2, January-February 2010, Pages 113-128.
15. Powrie HEG, Tasbaz OD, Wood RJK, Fisher CE. Performance of an electrostatic oil monitoring system during FZG gear scuffing test. In: Proceedings of the international conference on condition monitoring, 1999. p. 155–74.
16. T.J. Harvey, R.J.K. Wood, G. Denuault and H.E.G. Powrie, Effect of oil quality on electrostatic charge generation and transport, J. Electrostatics, 55(1), (2002) 1-23.
17. Harvey, T.J., Wood, R.J.K., Powrie, H.E.G. and Warrens, C., "Charging Ability of Pure Hydrocarbons and Lubricating Oils", Tribology Transactions, Volume 47, Number 2, April-June 2004, pages 263-271.
18. S. Morris, R.J.K. Wood, T.J. Harvey, H.E.G. Powrie, Use of Electrostatic Charge Monitoring for Early Detection of Adhesive Wear in Oil Lubricated Contacts, ASME Journal of Tribology 124(2) (2002), 288-296.
19. T.J. Harvey, S. Morris, R.J.K. Wood and H.E.G. Powrie, Real-Time Monitoring of Wear Debris Using Electrostatic Sensing Techniques, Proc. Instn. Mech. Engrs., Part J: Journal of Engineering Tribology, 221(J1) 2007, 27-40.
20. M. Zuercher, V. Heinzler, E. Schlücker, K. Esmaeili, T.J. Harvey, W. Holweger, L. Wang, Early failure detection for bearings in electrical environments, Processing the International Society for Condition Monitoring (ISCM) and the British Institute of Non-Destructive Testing (BINDT), 2017